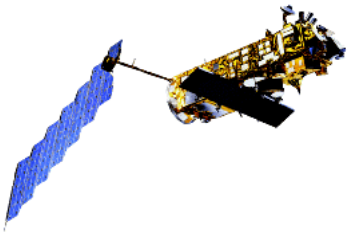

ENVISAT Microwave Radiometer Assessment Report

Cycle 086

11-01-2010 – 15-02-2010

(CCN No 1 to ESRIN Contract 21518/08/I-OL)

Prepared by :	B. PICARD, CLS M.-L. FRERY, CLS J.-R. DE BOER, CLS	
Checked by :	B. SOUSSI, CLS	
Approved by :	P. FEMENIAS, ESA	

CLS.DOS/NT/10-058
Edition 2.0, June 2010

Contents

List of Figures

Editing modifications

Version	Date	Object
1.0	February 2010	Creation of the document.
2.0	June 2010	Update of the time series.

1 Introduction

This document aims at reporting on the behavior of the ENVISAT Microwave Radiometer in terms of instrumental characteristics and quality of the brightness temperatures for cycle 086.
It is performed on the MWR level 1B data product. The decoding and pre-processing are done with the MWR level 1B reference processing chain located at CLS, using MWR level 0 data product as input (MWR_NL_OP). The data are from the ESA's ground stations in Kiruna, Sweden, and at ESRIN, Italy.

The objectives of this document are :

- To provide an instrumental status
- To check the stability of the instrument
- To report any change at the instrumental level likely to impact quality of the brightness temperatures

It is divided into the following topics:

- Synthesis of cycle 086 events and long term monitoring
- Significant events during cycle 086
- Long-term trends and former significant events

A specific topic is dedicated to the IPF version upgrade: **- Impact of the new calibration on radiometric data**

2 Synthesis

2.1 Conclusion for cycle 086

• New calibration coefficients are now applying in the radiometric model with the new versions of Level 1b processors.
• As expected, the impact of the new calibration coefficients is limited to the restitued gain of channel 36.5 GHz.
• The new versions of the ENVISAT Altimetry Level 1b and Level 2 Near Real Time (NRT) processing chains generating the FDGDR products (NRT IPF version 6.02L04) are operational since 7:30 UTC on 2 February 2010 (orbit 41443)
(from http://envisat.esa.int/earth/www/object/index.cfm?fobjectid=6776)
• The off-line (OFL) processing chain generating the IGDR products (NRT IPF version 6.02L04 and OFL CMA version 9.3) are operational since 4 February
(from http://envisat.esa.int/earth/www/object/index.cfm?fobjectid=6776).

2.2 Long term monitoring

The monitoring of the main instrumental parameters of the radiometer up to cycle 086 shows a drift of the 36.5 GHz channel. It appears that the gain, the sky horn counts, and the hot load counts have decreased between 3 and 29.30% since launch.

Two incidents occured during **cycle 84**:

- Problem with the data relay satellite ARTEMIS on 25th-26th November 2009
- ESRIN Antenna Failure on 9th November 2009.

One incident has occured during **cycle 80**:

- Unavailable MWR L0 data due to station acquisition problems and ARTEMIS unavailability which occured on 21st and 22th June 2009 respectively.

One incident has occured during **cycle 78**:

- Unavailable MWR L0 data, 32 complete orbits are missing due to instrument anomalies on 28-29 April and 11-12 May 2009.

Complete orbits are missing on **cycle 75**, mainly due to:

- Errors in the mission planning system which caused data not to be acquired
- Receiving stations and group segment facilities failures.

Two incidents occurs during the **cycle 71**:

- Unavailable MWR L0 data period in Kiruna station from 05/09/08 to 07/09/08
- A step is observed the 28 Aug 2008 on the hot counts, cold counts and residual temperature for the 36.5GHz channel.

Following a Payload HSM anomaly, no data are available from 17/01 8:50 to 17/01 18:41 during **cycle 65**.

Two planned unavailability periods occured during **cycle 64**:

- From 03 Dec 2007 22:00:00 (orbit 30115) to 04 Dec 2007 15:08:24 (orbit 30125) due to planned payload unavailability for OCM and maintenance
- From 13 Dec 2007 06:44:00 (orbit 30249) to 13 Dec 2007 12:25:49 (orbit = 30252) for memory maintenance

Following an anomaly within the on-ground mission control software, no data are available during the first four days of **cycle 62** (24/09 to 27/09).

Following an anomaly within the on-ground mission control software, no data are available during the last nine hours of the **cycle 61** (24/09/2007).

Due to Telemetry error during **cycle 60**, the data from 29/07 to 30/07 are missing. After a transition period, instrumental parameters are back to nearly nominal values.

An incident has occured during **cycle 58** between 26/05/2007 and 30/05/2007. After a short transition period, the data are back to nominal.

A big spike is also observed on 01/02/05 (**cycle 44**) for 23.8 GHz and 36.5 GHz channels.

A platform incident has occured during **cycle 46**, between 06/04/06 and 09/04/06.

The residual temperature is now 3.50 times higher in absolute value than the one estimated at the beginning of the mission and 4-6 times higher than the one expected from ground testing. No explanation was provided up to now. These features should impact the 36.5 GHz brightness temperature as reported in (Obligis et al, 2003). But as seen in the monitoring of the cold ocean brightness temperatures through the different previous reports the slope of the derived regression line varies at each cycle which makes the quantification of the real impact difficult since the variation observed on the cold TB is a combination of the instrumental features and the annual natural cycle.

The table below sums up main monitoring anomalies observed since ENVISAT cycle 36 :

CycleNumber	Type of event	Date	Impacted Monitoring parameters
86	New IPF	02/02/10 (FDGDR, pass 41443) and 04/02/10 (IGDR, pass 41451)	new versions of IPF (6.02L04) and CMA (9.3) including new calibration coefficients. Limited impact on 36.5 GHz restitued gain.
84	Unavailbility	09/11/09 and 25/11/09	Problem with data relay satellite ARTEMIS and ASRIN Antenna failure
80	Unavailability	21/06/09 and 22/06/09	Unavailable MWR L0 data due to station acquisition problems and ARTEMIS unavailability
78	Unavailability	28/04/09 to 29/04/09 and 11/05/09 to 12/05/09	Unavailable MWR L0 data, 32 complete orbits are missing
77	Unavailability	16/03/09 and 19/03/09	Unavailable MWR L0 data, two complete orbits are missing and bad antenna acquisition
75	Unavailability	22/12/08 to 26/01/09	Complete orbits are missing
74	Unavailability	14/12/08 to 17/12/08	Unavailable MWR L0 data due to operational problems
71	Quality	28/08/08	Cold counts, hot counts and residual temperature step down for 36.5GHz channel
71	Unavailability	05/09/08 to 07/09/08	Unavailable L0 MWR data period
65	Unavailability	17/01/08 to 17/01/08	Payload HSM anomaly
64	Unavailability	13/12/07 to 13/12/07	Planned unavailability for memory maintenance
64	Unavailability	03/12/07 to 04/12/07	Planned payload unavailability for OCM and maintenance
62	Unavailability	24/09/07 to 27/09/07	Unavailable L0 MWR data period. (anomaly within the on-ground mission control software)
61	Unavailability	24/09/07 to 24/09/07	Unavailable L0 MWR data period. (anomaly within the on-ground mission control software)
60	Unavailability	29/07/07 to 30/07/07	Unavailable L0 MWR data period. (Telemetry error)
58	Unavailability	26/05/07 to 30/05/07	MWR switched to Standby/Refuse mode after CEU (Central Electronic Unit) temperature uniformity flag was set to one. The situation was back to nominal after a COLD RESET of the DORIS/MWR ICU

continued on next page

continued from previous page

CycleNumber	Type of event	Date	Impacted Monitoring parameters
53	Unavaibility	30/11/06 and 15/12/06	Two unavailable L0 MWR data periods.
51	Unavaibility	26/09/06 to 01/10/06	Unavailable L0 MWR data period.
51	Unavaibility	07/09/06 to 11/09/06	Unavailable L0 MWR data period.
46	Quality	09/04/06	Gain loss, sky horn counts and hot load counts spikes for both channels.
44	Quality	01/02/06	Big spike on gain and TE values for both channels.
41	Quality	21/09/05	Spike on cold ocean TB values for both channels.
36	Quality	24/04/05	Gain values and sky horn counts step down for 36.5 GHz channel.

Table 1: **Main monitoring anomalies observed from cycle 36**

3 Significant events during cycle 086

To monitor the instrument behaviour during its lifetime, the key parameters are plotted **in figures 1, 2 and 3**: gain (after correction of the thermal variations, modeled as a parabolic function), hot load and sky horn counts, and the residual term TE (residual temperature contribution due to errors in the estimated coefficients). The instrument stability is ensured if none of these parameters do vary with time (see the following paragraphs 3.1, 3.2 and 3.3).

On the other hand, to assess the long term stability of the MWR radiometer, a monitoring of the two brightness temperatures was performed by selecting the coldest measurements over ocean, as shown in **figure 4**. This method, derived from Ruf's one for TMR (Ruf, 2000), was found to be the most efficient to point out the slight trend of the ERS2 23.8 GHz channel (Eymard et Obligis, 1999; Eymard et al, 2002) (see the following paragraph 3.4).

3.1 Gain survey

Figure 1 represents the gains of the two channels 23.8 and 36.5 GHz on the last three cycles.

The updated total decrease on channel 2 (36.5 GHz) is about 29.30% (from 10.4 at the beginning to about 7.353 now).

No particular event during this cycle 086.

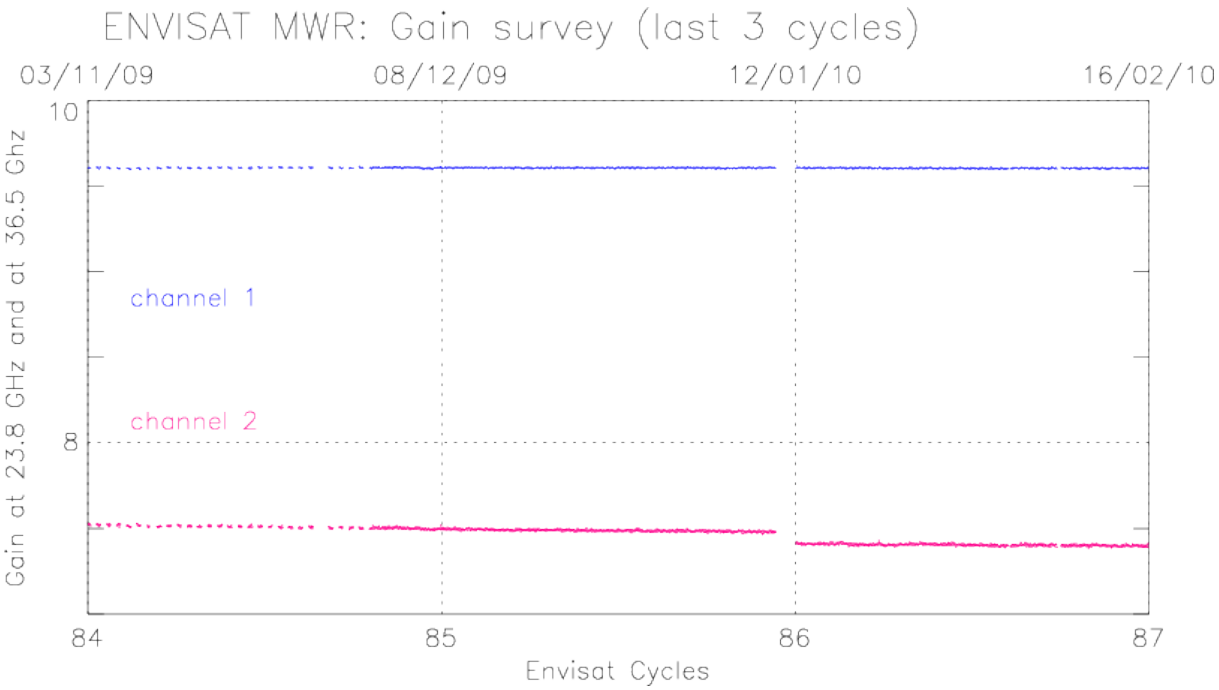

Figure 1: Time evolution of the gain (zoom on the last 3 cycles).

3.2 Sky horn and hot load counts survey

No particular event during this cycle 086.

Figure 2 represents the counts of the two channels 23.8 and 36.5 GHz for the sky horn (top), and for the hot load (bottom).

The updated total decrease of sky horn counts on channel 2 (36.5 GHz) is about -24.78% (from 3600 at the beginning to about 2708 now).

The updated total decrease of hot load counts on channel 2 (36.5 GHz) is about -5.61% (from 660 at the beginning to about 623 now).

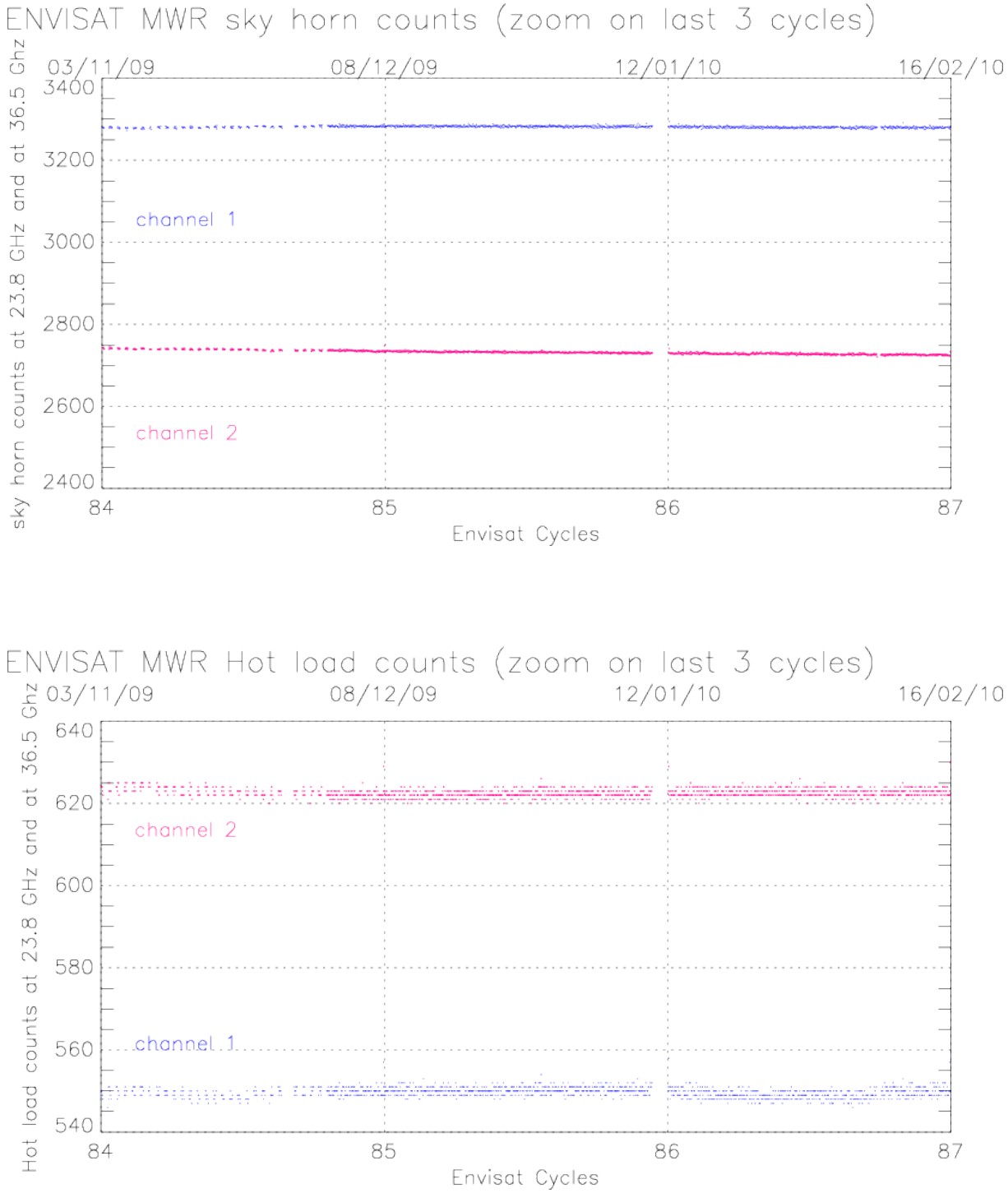

Figure 2: Time evolution of the sky horn (top) and hot load (bottom) counts (zoom on the last 3 cycles).

3.3 Residual temperature survey

No particular event during this cycle 086.

Figure 3 represents the residual temperature of the two channels 23.8 and 36.5 GHz since Envisat launch (top), and on the last three cycles (bottom).

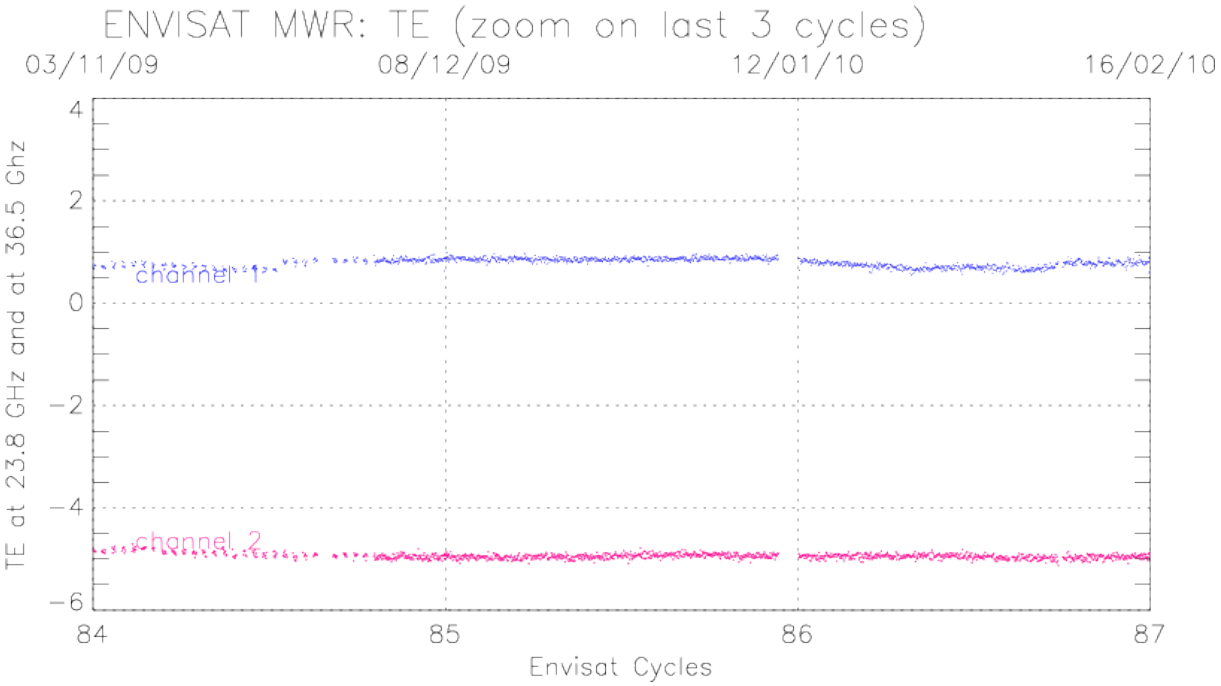

Figure 3: Time evolution of the residual temperature TE (zoom on the last 3 cycles).

3.4 Cold ocean Tb monitoring

Following the method explained above and using a threshold equal to the average minus the standard deviation, the Envisat resulting time series is plotted, after a 90-days running average, in **figure 4**. This running average leads to a small delay between the current cycle and the last available values of the cold ocean Tb monitoring.

For the first channel, the cold ocean TB values present a -0.0291 K/year variation, while a variation of -0.008 K/year is observed for the second one.

On both channels, the cold ocean Tb are the most cold from cycle 29 to cycle 52 for the 23.8 GHz channel and from cycle 43 to cycle 52 for the 36.5 GHz channel (apart from the stabilization period, cycle 4 to 16). Since this phenomenon is observed on both channels, a geophysical origin is considered.

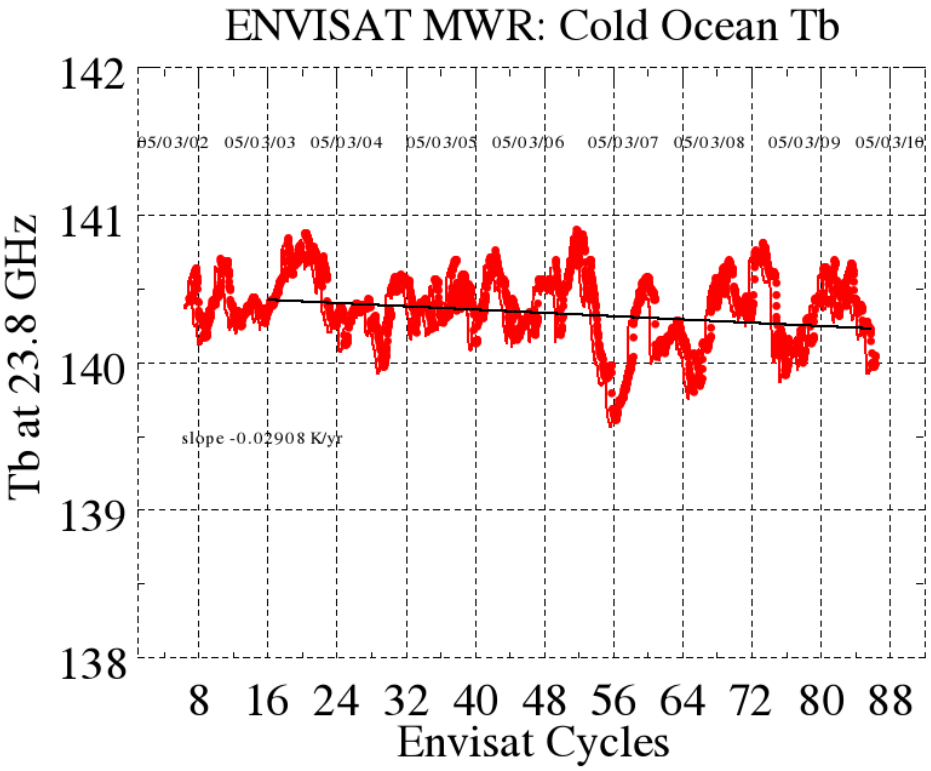

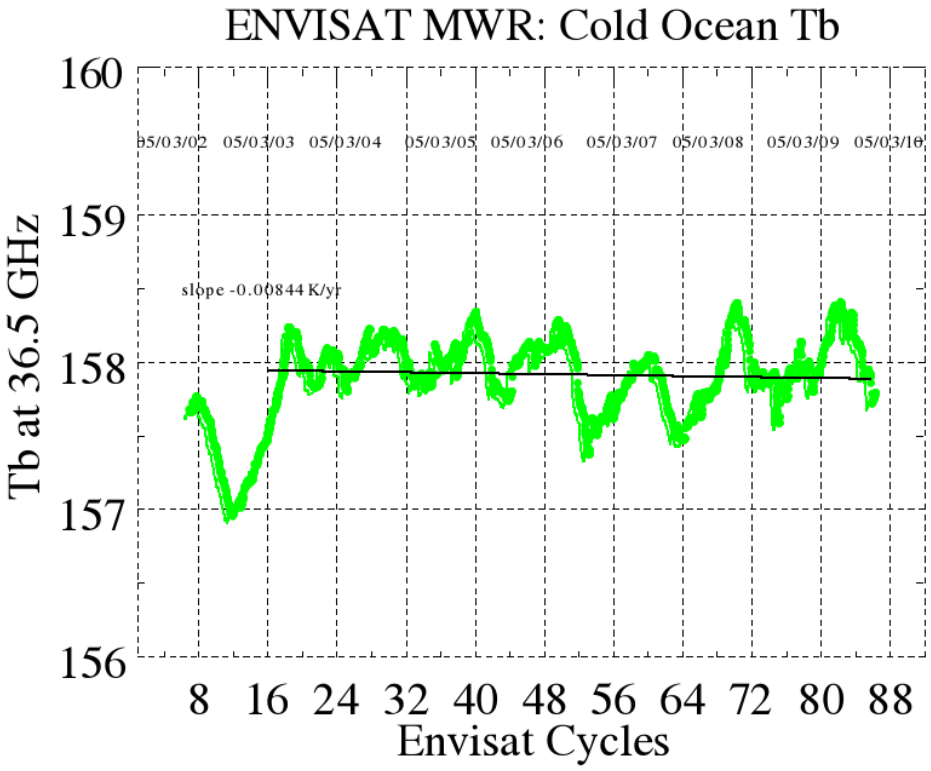

Figure 4: Cold Ocean brightness temperature for the 23.8 Ghz channel (top) and the 36.5 GHz channel (bottom) (90 days running average).

4 Long-term trends and former significant events

4.1 Gain survey

Figure 5 shows that the gain in the 23.8 GHz channel remains stable around 9.6. For the second channel, the evolution shows two decreasing trends, small at the beginning and a stronger one since cycle 8. The total decrease is about 29.30% (at 10.4 at the beginning and about 7.353 now).

Two incidents occured during **cycle 84**: Problem with the data relay satellite ARTEMIS on 25th-26th November 2009 ESRIN Antenna Failure on 9th November 2009.
One incident has occured during **cycle 80**, unavailable MWR L0 data due to station acquisition problems and ARTEMIS unavailability which occured on 21st and 22th June 2009 respectively.
One incident has occured during **cycle 78**,unavailable MWR L0 data,32 complete orbits are missing due to instrument anomalies on 28-29 April and 11-12 May 2009.
One incident has occured during this **cycle 75**, complete orbits are missing, mainly due errors in the mission planning system which caused data not to be acquired and receiving stations and group segment facilities failures.
During **cycle 71**, no L0 MWR data are available in Kiruna station from the 05 Sep 2008 to 07 Sept 2008
Following a Payload HSM anomaly, no data are available from 17/01 8:50 to 17/01 18:41 during **cycle 65** with no particular impact on the gain.
Two planned unavailability periods (03/12 to 04/12 and 13/12 from 6 am to 12 am) during the **cycle 64** with no particular impact on the gain.
Following an anomaly within the on-ground mission control software, no data are available during the first four days of **cycle 62** (24/09 to 27/09). After a short transition period, the gain has regained nominal values.
Following an anomaly within the on-ground mission control software, no data are available during the last nine hours of the **cycle 61** (24/09/2007).
Due to Telemetry error during **cycle 60**, the data from 29/07 to 30/07 are missing. After a transition period, instrumental parameters are back to nearly nominal values.
An incident has occured during **cycle 58** between 26/05/2007 and 30/05/2007. After a short transition period, the data are back to nominal.
A plateform deficiency has occured from 06/04/06 to 09/04/06 (**cycle 46**). Then, gain loss is observed for both channels on figures. A spike is also observed on 14/04/06 for both channels.
For cycle 45, a slight jump in the very last days of **cycle 45** is observed.
A big spike occurs on 01/02/06 during **cycle 44** for both channels.
Note that a step down on the gain values occurs during **cycle 36** for 36.5 GHz channel.

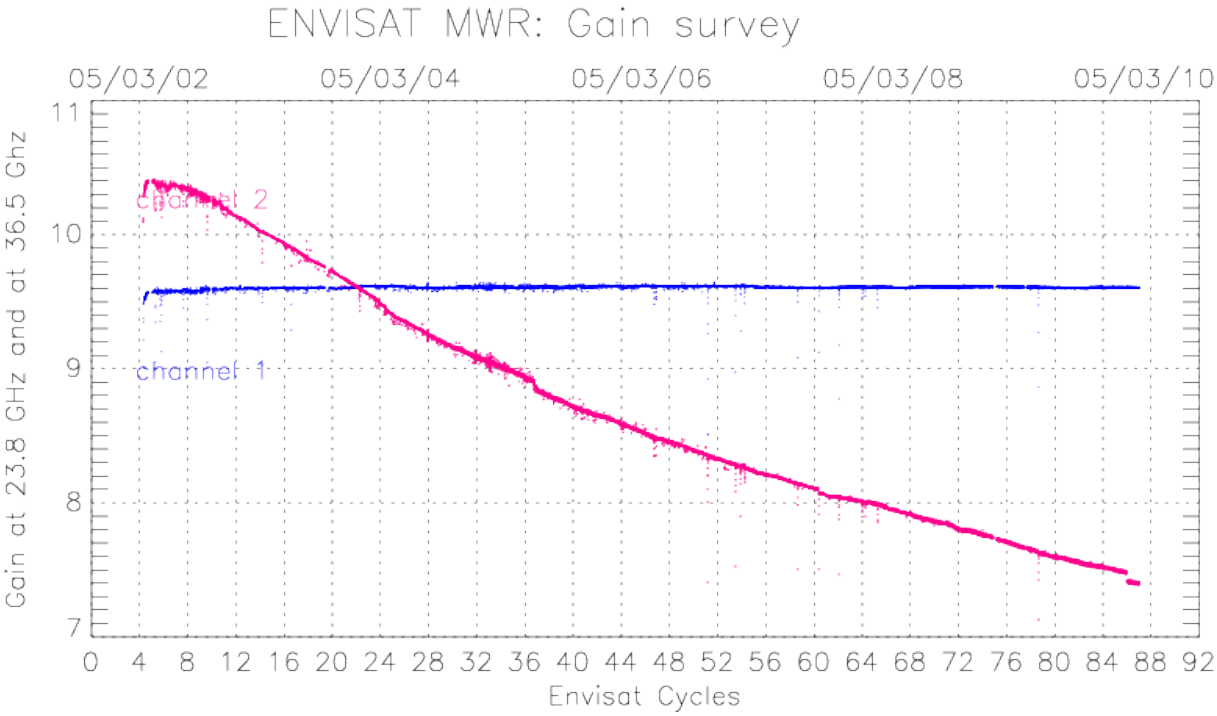

Figure 5: Time evolution of the gain since Envisat launch.

4.2 Sky horn and hot load counts survey

The sky horn counts on **figure 6** exhibit similar features than the gain for both channels. The counts present a very slight increase with time for the first channel. For the second one, the values drop from 3600 to 2708 (-24.78%).

The hot load counts on the same figure are stable for the first channel, around 553. They decrease for the second channel from 660 at launch time to about 636 (-3.64%).

Two incidents occured during **cycle 84**: Problem with the data relay satellite ARTEMIS on 25th-26th November 2009 ESRIN Antenna Failure on 9th November 2009.
One incident has occured during **cycle 80**, unavailable MWR L0 data due to station acquisition problems and ARTEMIS unavailability which occured on 21st and 22th June 2009 respectively.
One incident has occured during **cycle 78**,unavailable MWR L0 data,32 complete orbits are missing due to instrument anomalies on 28-29 April and 11-12 May 2009.
One incident has occured during this **cycle 75**, complete orbits are missing, mainly due errors in the mission planning system which caused data not to be acquired and receiving stations and group segment facilities failures.
During this **cycle 71**, no L0 MWR data are available in Kiruna station from the 05 Sep 2008 to 07 Sept 2008. A step down is observed for the hot and cold counts of the 36.5 GHz channel.
Following a Payload HSM anomaly, no data are available from 17/01 8:50 to 17/01 18:41 during **cycle 65** which results on a small jump on hot load counts for channel 2.
Two planned unavailability periods (03/12 to 04/12 and 13/12 from 6 am to 12 am) during this cycle 64. Following the first unavailability period, a small drop on sky horn counts (both channels) is observed just as, on hot load counts, a drop for channel 1 and a descreasing slope for channel 2. Note that the drop on hot load counts for channel 1 almost balances the jump that has occured after the incident at the beginning of **cycle 62**.
Following an anomaly within the on-ground mission control software, no data are available during the first four days of cycle 62 (24/09 to 27/09). After a short transition period, the counts have regained nominal values except for the hot load counts on channel 1 which seems to be stabilized at larger values.
Following an anomaly within the on-ground mission control software, no data are available during the last nine hours of the **cycle 61** (24/09/2007).
Due to Telemetry error during **cycle 60**, the data from 29/07 to 30/07 are missing. After a transition period, instrumental parameters are back to nearly nominal values.
An incident has occured during **cycle 58** between 26/05/2007 and 30/05/2007. After a short transition period, the data are back to nominal.
Note that spikes observed between 09/04/06 and 14/04/06 (**cycle 46**) are related to gain incidents invoked above.
A slight increase of hot load counts is observed in the very last days of **cycle 45** for first channel, while, for the second one, the increase is observed since the early days of this cycle.

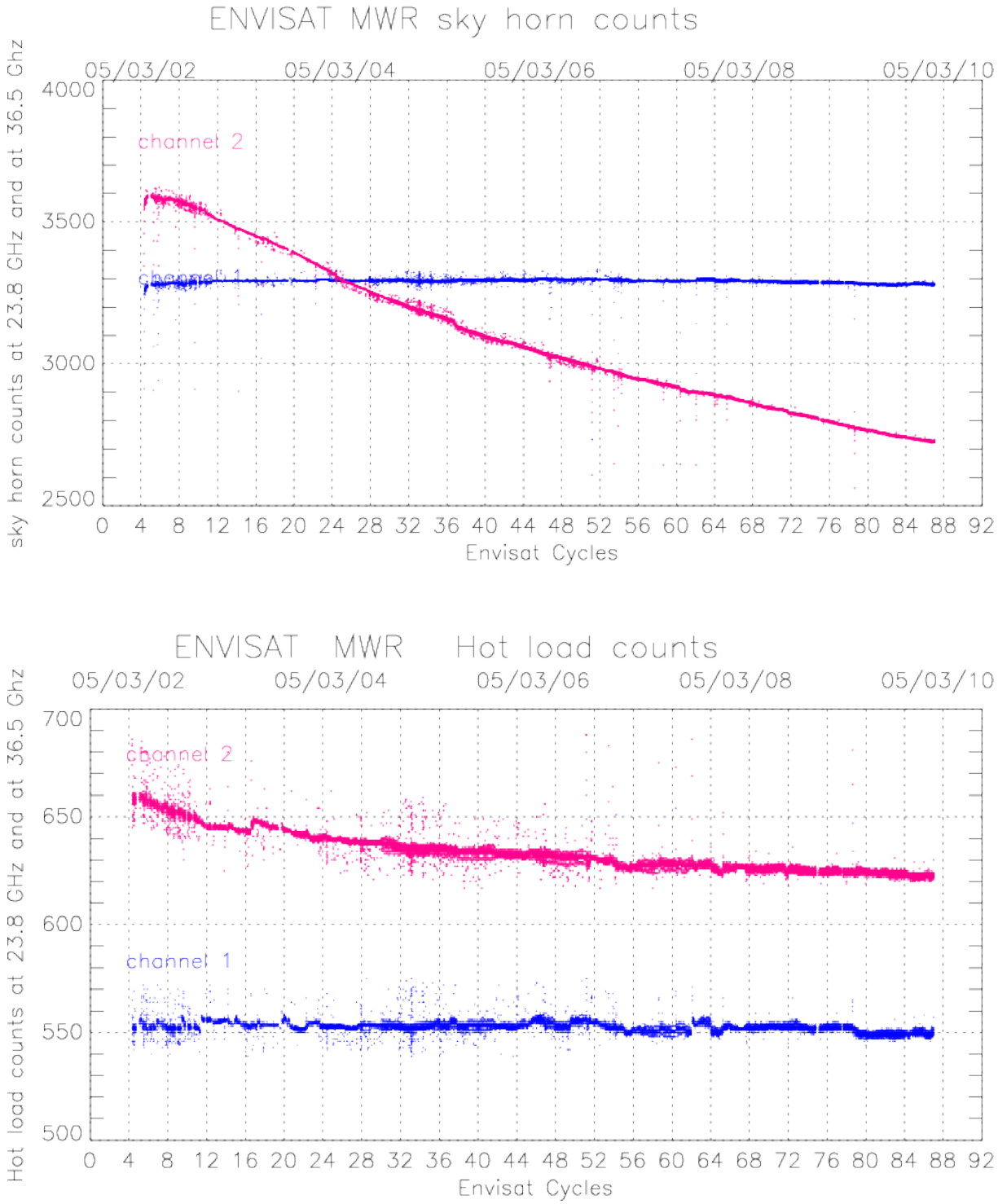

Figure 6: Time evolution of the sky horn (top) and hot load (bottom) counts since Envisat launch.

4.3 Residual temperature survey

Figure 7 shows the residual temperature. Since launch, the values are higher than evaluated from ground testing. The residual temperature was expected to be around 0.5 K for the first channel and a bit higher, 0.5-0.7 K for the second one, i.e. close to the ERS ones (Eymard et al, 2002).

Two incidents occured during **cycle 84**: Problem with the data relay satellite ARTEMIS on 25th-26th November 2009 ESRIN Antenna Failure on 9th November 2009.
One incident has occured during **cycle 80**, unavailable MWR L0 data due to station acquisition problems and ARTEMIS unavailability which occured on 21st and 22th June 2009 respectively.
One incident has occured during **cycle 78**,unavailable MWR L0 data,32 complete orbits are missing due to instrument anomalies on 28-29 April and 11-12 May 2009.
One incident has occured during this **cycle 75**, complete orbits are missing, mainly due errors in the mission planning system which caused data not to be acquired and receiving stations and group segment facilities failures.
During **cycle 71**, no MWR L0 dataare available in Kiruna station from the 05 Sep 2008 to 07 Sept 2008.
Following a Payload HSM anomaly, no data are available from 17/01 8:50 to 17/01 18:41 during **cycle 65** which results on a small jump on residual temperature for channel 2.
Two planned unavailability periods (3/12 to 4/12 and 13/12 from 6 am to 12 am) during this cycle 64. Following the first unavailability period, a drop for channel 1 (-0.5 K) and a decreasing slope for channel 2 are observed. The drop on channel 1 seems to almost balance the jump of 0.5 K that occured after the incident at the beginning of **cycle 62.**
Following an anomaly within the on-ground mission control software, no data are available during the first four days of **cycle 62** (24/09 to 27/09). After a short transition period, the residual temperature has regained nominal values on channel 2 but seems to be stabilized at larger values on channel 1.
Following an anomaly within the on-ground mission control software, no data are available during the last nine hours of the **cycle 61** (24/09/2007).
Due to Telemetry error during **cycle 60**, the data from 29/07 to 30/07 are missing. After a transition period, instrumental parameters are back to nearly nominal values.
An incident has occured during **cycle 58** between 26/05/2007 and 30/05/2007. After a short transition period, the data are back to nominal.
Note that a big spike on 01/02/06 (**cycle 44**) for both channels are observed, as it is on gain values.
A residual temperature increase is observed after this spike for channel 1, during (**cycle 45**).
There are 4 particular features of this parameter to analyse:

- a drift of the residual temperature at 36.5 GHz, the values were down to -2.5 K with a regular linear decrease since 2-3 months after launch to cycle 16.
- a step is then observed with an increase of 0.5 K. The values were around -2.0 K and are decreasing again and are around -3.60 K.
- a step is observed at 23.8 GHz during cycle 11 with an increase of 0.5 K.
- a decrease is observed after the previous mentionned step for the 23.8 GHz channel. Since cycle 16, the values vary around 1.

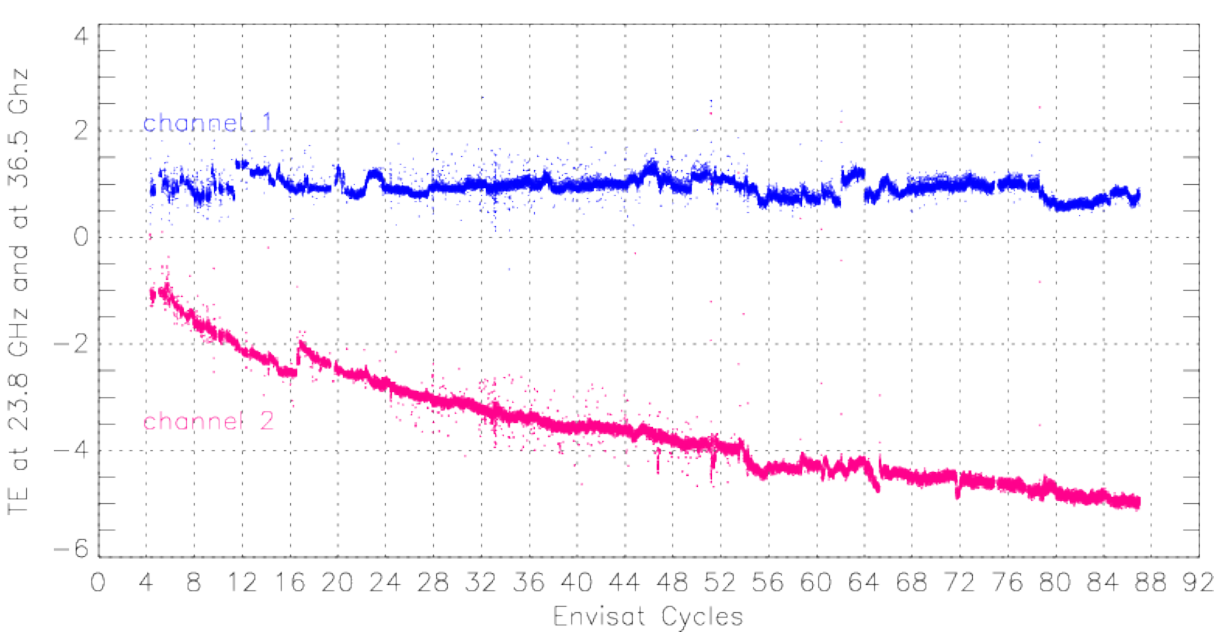

Figure 7: Time evolution of the residual temperature TE since Envisat launch.

5 Impact of the new calibration on radiometric data

Amongst various improvements, the new IPF 6.02 version includes updated values for the radiometer calibration coefficients (L1B) but also for the neural network parameters (L2).

We propose to quantify the impact of this calibration of the radiometer parameters from L1 to L2. The results presented in the following are extracted from the reprocessing of cycle 85.

Geophysical L2 products retrieved from radiometric measurements, including the wet tropospheric correction, are estimated by use of a neural network, from a simulated dataset of brightness temperatures. These TB are simulated by means of a radiative transfer model from ECWF surface fields.

Then, the final quality of these products lies mainly on the consistency between the measured TB and the learning dataset of simulated TB.

This consistency is driven on one hand by the ageing of the instrument and on the improvement of ECWMF modeling on the other hand. A first calibration of the Envisat/MWR was performed in October 2002. Since this period, significant improvements occurred in the ECMWF meteorological model (assimilation of new data, improvements in the assimilation scheme). In order to benefit from these improvements, a new calibration has been proposed and has been implemented in the IPF 6.02.

5.1 Expected Impacts

A specific technical note dedicated to the impact of the new calibration has been written in 2007 in the frame of the CCN 5 of the contract RA-2 ocean and MWR measurement performance long-term monitoring 17293/03/I-OL [9]. The following remarks and figures are extracted from this note.

5.1.1 On level 1B products

The values for two instrumental parameters are updated (one value for each channel): the transmission coefficient of the reflector (η_ref) and the sky horn feed transmission coefficient (a_cc) (see Tab. 1).

Table 2: Previous (OLD) and updated (NEW) values for the calibration parameters.

	23.8 GHz		36.5 GHz	
	OLD	NEW	OLD	NEW
η_ref	0.99	0.984	0.999	0.988
a_cc	1.01	1.01	1.04	1.05

The sky horn feed transmission coefficient (a_cc) has a direct but weak impact on the estimation of the restitued gain (see Fig. 8), and, indirectly through this gain, on the residual temperature (see Fig. 9). Note that a_cc is not modified for the channel 23.8 GHz: the new calibration has no impact on the gain and on the residual temperature of this channel.

The transmission coefficient of the reflector (η_ref) is involved in the computation of the side-lobe correction (see Fig. 10) and has a stronger impact on the brightess temperature.

$$\begin{cases} G\_channel1 = \dfrac{Hotload1 - skyhorn1}{T\_RF1} \\ G\_channel2 = \dfrac{Hotload2 - Skyhorn2}{T\_RF2} \end{cases} \qquad \text{Eq 5.1.3.2.3-4}$$

here called "Calibration Gain Evaluation" where

$$T\_fc1 = [a\_cc \cdot Tsh1 + (1 - a\_cc)T\_cc]a\_cw + (1 - a\_cw)T\_cw \qquad \text{Eq 5.1.3.2.3-5}$$

$$T\_fc2 = [a\_cc \cdot Tsh2 + (1 - a\_cc)T\_cc]a\_cw + (1 - a\_cw)T\_cw \qquad \text{Eq 5.1.3.2.3-6}$$

and where T_RF1 and T_RF2 are the temperature at the receiver input described by

$$T\_RF1 = c\_h \cdot T\_h1 + c\_fc \cdot T\_fc1 + c\_hc \cdot T\_hc1$$

$$T\_RF2 = c\_h \cdot T\_h2 + c\_fc \cdot T\_fc2 + c\_hc \cdot T\_hc2 \qquad \text{Eq 5.1.3.2.3-7}$$

Figure 8: Estimation of the gain

$$\begin{cases} TE\_channel1 = \dfrac{Hotload1 - offset1}{G\_channel1} - a\_ref \cdot Tref1 - a\_D \cdot T\_D1 - a2 \cdot T\_fc + a3 \cdot T\_hc1 + a4 \cdot T\_h1 + a6 \cdot T\_cal1 + a50 \\ TE\_channel2 = \dfrac{Hotload2 - offset2}{G\_channel2} - a\_ref \cdot Tref2 - a\_D \cdot T\_D2 - a2 \cdot T\_fc + a3 \cdot T\_hc2 + a4 \cdot T\_h2 + a6 \cdot T\_cal2 + a50 \end{cases}$$

Eq 5.1.3.2.3-9

Figure 9: Estimation of the residual temperature

tslg_24 = eta_refl_24*tsl_24 + (1-eta_refl_24)*Trefl Eq 5.1.3.4.2-11

tslg_36 = eta_refl_36*tsl_36 + (1-eta_refl_36)*Trefl Eq 5.1.3.4.2-12

The brightness temperature for each channel is then evaluated:

Tb24 = (TA_channel1 - tslg_24)/(eta_refl_24*beam_eff_24)Eq 5.1.3.4.2-13

Tb36 = (TA_channel2 - tslg_36)/(eta_refl_36*beam_eff_36)Eq 5.1.3.4.2-14

Figure 10: Computation of side-lobe correction

Figures 11 and 12 show the scatterplots of the measured TB against the simulated ones for the two channels, respectively before and after the new calibration.

Comparing the statistics, the expected impact on the brightess temperature is a drop on the mean value of about 0.5 K on channel 23.8 GHz and about 2 K on channel 36.5 GHz.

The standart deviation could be slightly increased by 0.04 K on channel 1 and 0.2 K on channel 2.

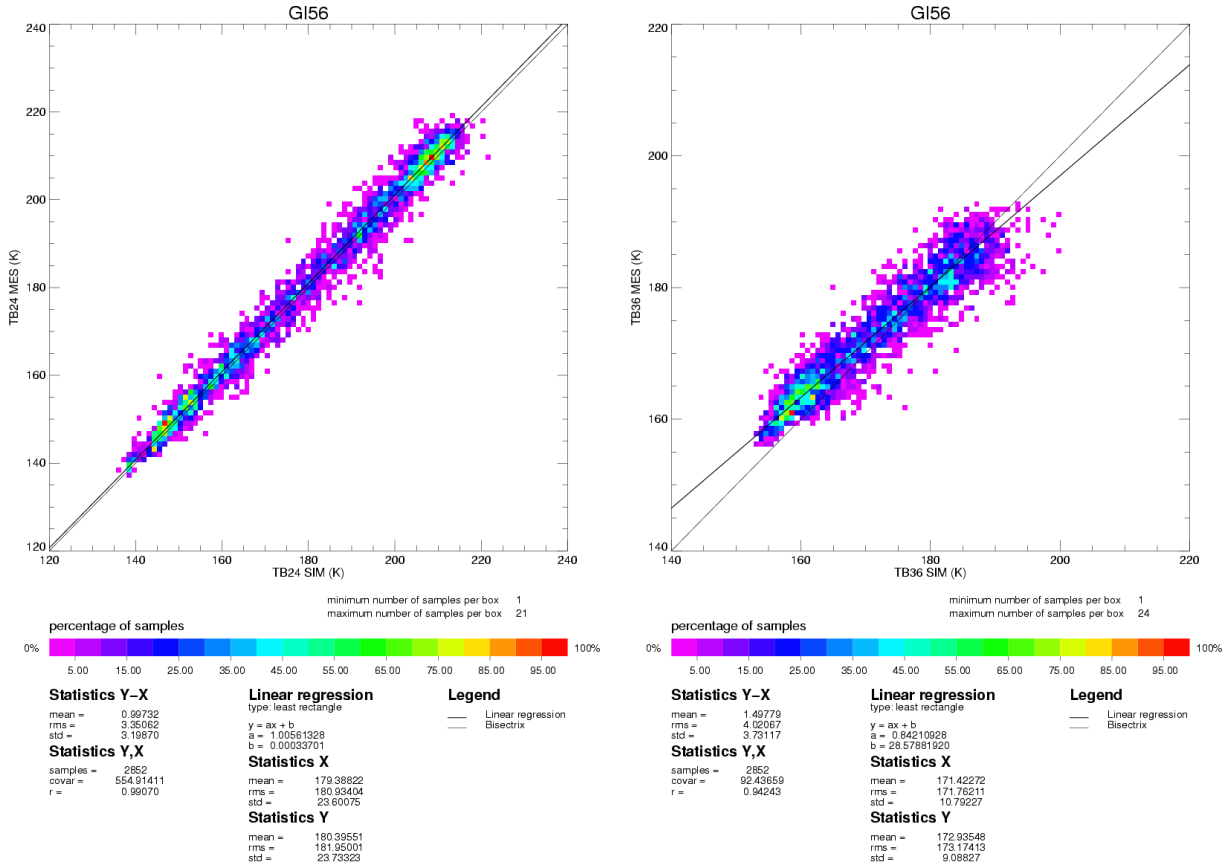

Figure 11: Scatterplot between simulated TB and measured TB before the new calibration: 23.8 GHz (left) and 36.5 GHz (right)

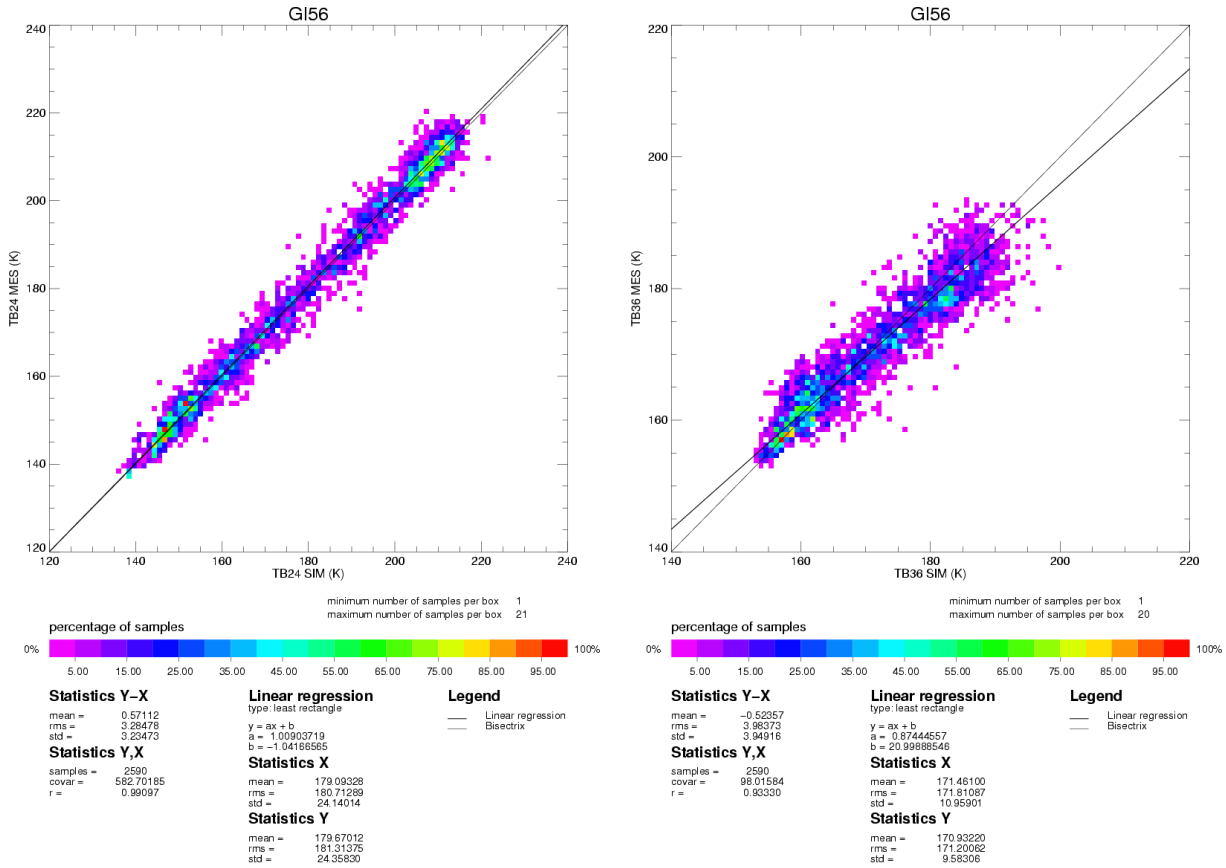

Figure 12: Scatterplot between simulated TB and measured TB after the new calibration: 23.8 GHz (left) and 36.5 GHz (right)

5.1.2 On the wet tropospheric correction

Using newly calibrated TB, the performance of the neural network parameterized with updated coefficients is expected to be very good.

Figure 13 shows a scatterplot of restitued dh from radiometric measurements with the new calibration against ECMWF one.

The expected bias between the radiometer retrieval and the model is close to 4.4 mm with an rms of 1.76 cm after the new calibration.

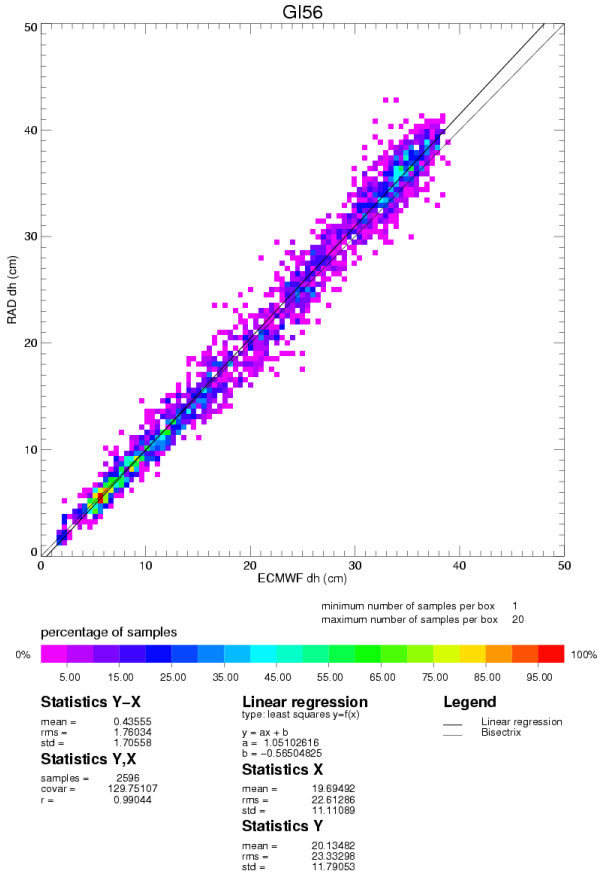

Figure 13: Scatterplot between ECMWF dh and restitued dh from radiometric measurements after the new calibration: expected impact

5.2 Actual Impacts

The results presented in the following are extracted from the reprocessing of cycle 85.

5.2.1 On level 1 data

Level 1 data are used for expertise activities only and consist on a record of the gain and the residual temperature used to compute the antenna temperature.

As expected, there is no impact of the new calibration on the 23.8 GHz Level 1 data.

Mainly, the updated values of the 36.5 GHz L1 parameters are biased when compared to the values for the previous version of the IPF (see Fig .14).

The impact on the gain is -6.85 mV/K and -0.022 K on the residual temperature.

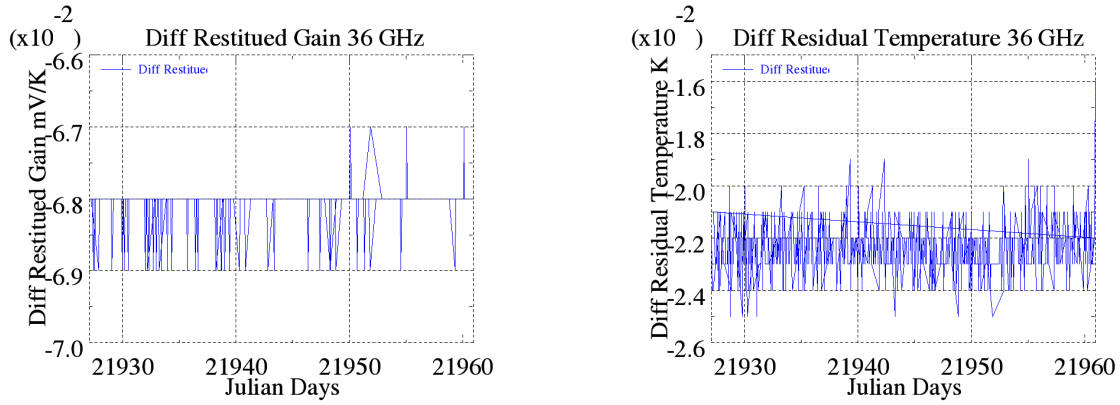

Figure 14: Impact of the new calibration on Level 1 data

5.2.2 On level 1B products

Figures 15 and 16 show the scatterplots of the newly calibrated TB against the old ones for the two channels, respectively on open ocean and over all type of surfaces.

The statistics of Figure 15 show a mean difference between the datasets of about 0.9 K (0.5 K expected) and 2.7 K (2 K expected) respectively for the channel 23.8 GHz and the channel 36.5 GHz.

The standart deviation of the difference is about 0.34 K (0.04 K expected) for the channel 23.8 GHz and 0.47 K (0.2 K expected) for the channel 36.5 GHz.

The difference between the actual statistics and the expected ones could be explained by the availability of only one cycle for the reprocessed data as the expected statistics are performed over one year of data.

Considering this, we could assume that the actual bias between the old dataset and the newly calibrated TB is in conformity with the expectations and that the standard deviation of the difference would be reduced with a larger amount of reprocessed data. This is to be confirmed all along the reprocessing.

The statistics over all type of surfaces (see Figure 16) show a smaller bias between calibrated and non-calibrated TB of about 0.7 K and 2.11 K and a larger standart deviation of 0.44 K and 0.58 K, respectively for the channel 23.8 GHz and the channel 36.5 GHz respectively.

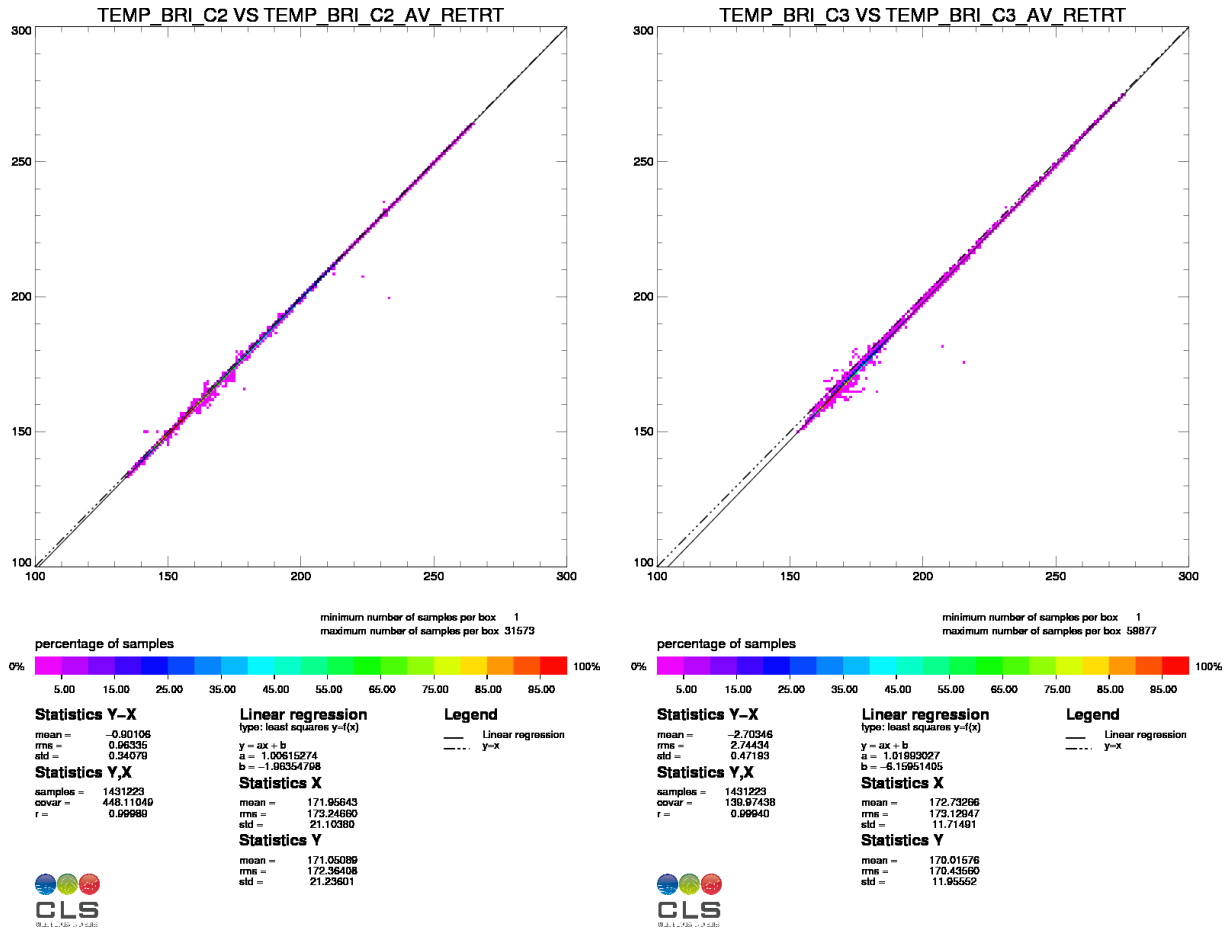

Figure 15: Impact of the new calibration on the brightness temperatures: open ocean

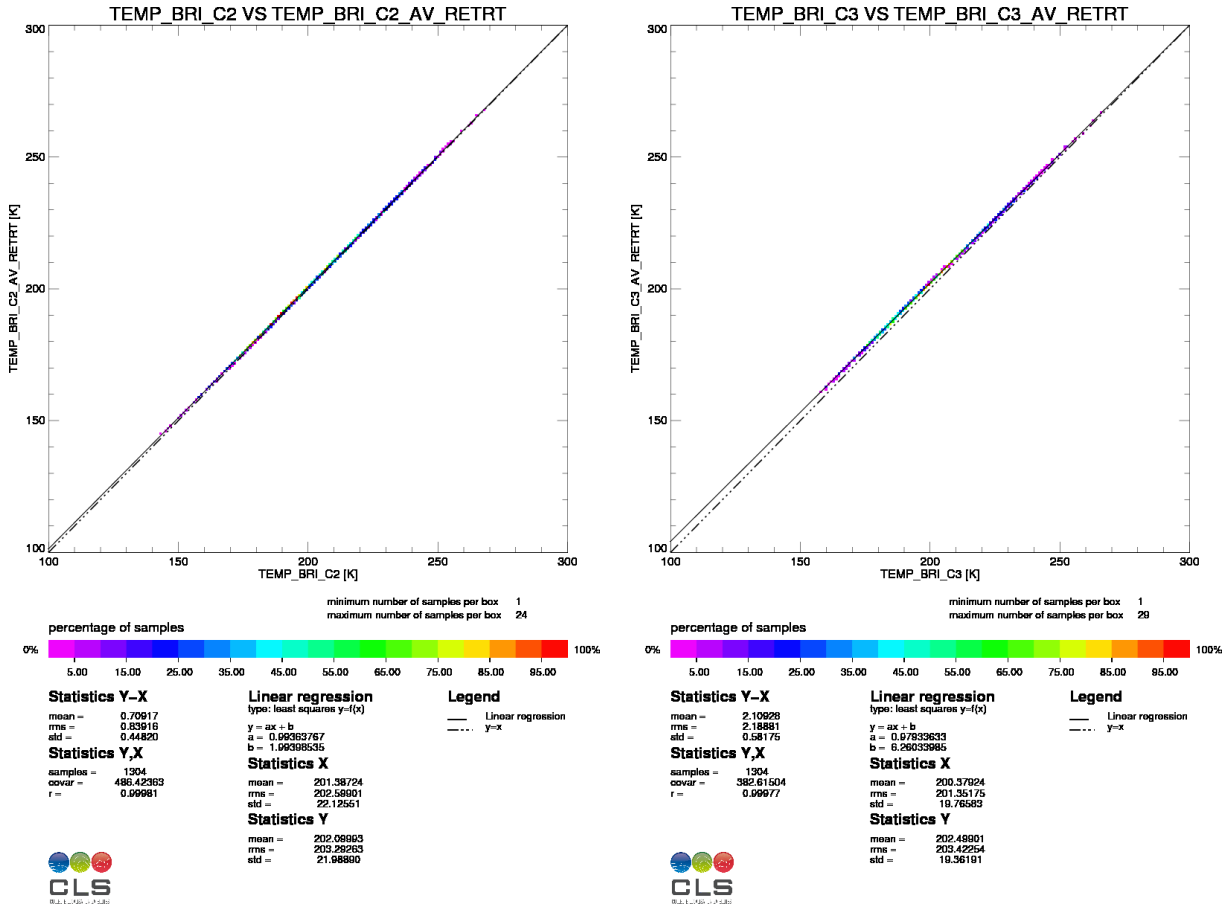

Figure 16: Impact of the new calibration on the brightness temperatures: all type of surfaces

5.2.3 On level 2 products

Figure 17 shows a scatterplot of the restitued dh from radiometric measurements with the new calibration against the restitued dh from radiometric measurements before the new calibration.

The impact is very weak with in terms of bias (less than 0.3 mm). Nothe that the standart deviation is of about 1 cm.

Figure 18 shows a scatterplot of the restitued dh from radiometric measurements with the new calibration against ECMWF one.

The bias between the radiometer retrieval and the model is close to 5.6 mm (4.4 mm expected) with an rms of 2.0 cm (1.75 cm expected) after the new calibration.

As for the brightness temperature, we could assume that the actual bias between the old dataset and the dh estimated with newly calibrated TB is in conformity with the expectations. This is to be confirmed all along the reprocessing.

Obviously, the improvement of the new calibration onto the quality of the L2 data will be fully quantified when a sufficient amount of data will be acquired and will not be limited only to a reduction of the bias between the radiometer and the model.

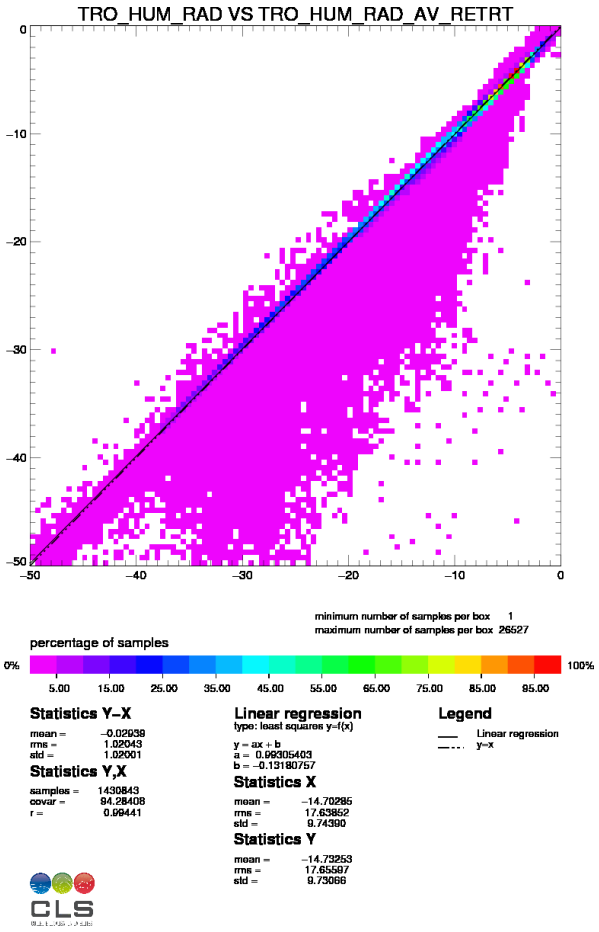

Figure 17: Impact of the new calibration on the wet tropospheric correction

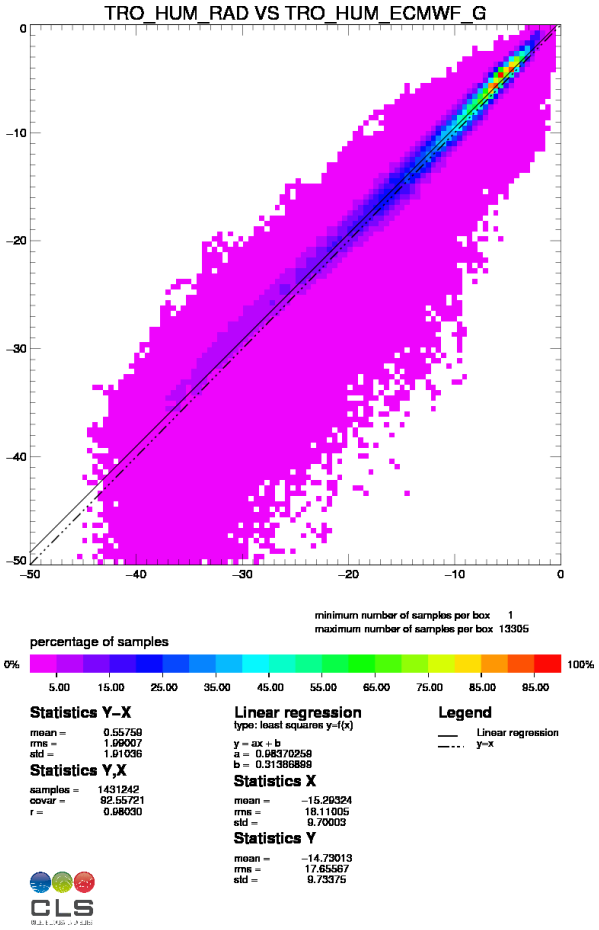

Figure 18: Scatterplot between ECMWF dh and restitued dh from radiometric measurements after the new calibration.

5.3 Conclusion

The new IPF 6.02 version includes updated values for the radiometer calibration coefficients (L1B) but also for the neural network parameters (L2).

The values for two instrumental parameters are updated (one value for each channel): the transmission coefficient of the reflector (η_ref) and the sky horn feed transmission coefficient (a_cc).

The sky horn feed transmission coefficient (a_cc) has a direct but weak impact on the estimation of the restitued gain and, indirectly through this gain, on the residual temperature.

The transmission coefficient of the reflector (η_ref) is involved in the computation of the side-lobe correction and has a stronger impact on the brightess temperature.

As expected, there is no impact of the new calibration on the 23.8 GHz Level 1 data and the impact on the gain is -6.85 mV/K and -0.022 K on the residual temperature for the 36.5 GHz channel.

The statistics on the brightness temperatures show a mean difference between the new and the old datasets of about 0.9 K (0.5 K expected) and 2.7 K (2 K expected) respectively for the channel 23.8 GHz and the channel 36.5 GHz.

The bias between the radiometer retrieval and the model is close to 5.6 mm (4.4 mm expected) with an rms of 2.0 cm (1.75 cm expected) after the new calibration.

The difference between the actual statistics and the expected ones could be explained by the availability of only one cycle for the reprocessed data as the expected statistics are performed over one year of data.

We could assume that the actual bias estimated between data before and after the calibration is in conformity with the expectations. This is to be confirmed all along the reprocessing.

Obviously, the improvement of the new calibration onto the quality of the L2 data will be fully

quantified when a sufficient amount of data will be acquired and will not be limited only to a reduction of the bias between the radiometer and the model.

A Monitoring of the radiometer internal parameters

The radiometer telemetry primarily contains the radiometer counts for each channel, which are related to the brightness temperatures of the main antenna and the two calibration loads, through the working model (Bernard et al, 1993) summarized below:

$$\mathbf{Tfc} = acc\ ah0\ \mathbf{TC} + (1 - acc)\ ah0\ \mathbf{Tcc} + (1 - ah0)\mathbf{Th}$$

$$\mathbf{G} = (Cc - Cf)/[ao + af\ \mathbf{Tfc} - ac\ \mathbf{Tc} + ah\ \mathbf{Th/c}]$$

$$\mathbf{TE} = (Cc - off)/\mathbf{G} - aref\ \mathbf{Tref} - ad\ \mathbf{Td} + a2\ \mathbf{Tfc} + a3\ \mathbf{Th/c} + a4\ \mathbf{Tc} + a6\ \mathbf{Tcal} + a5$$

$$\mathbf{T'a} = b1\ \mathbf{Tref} + b2\ \mathbf{Td} - b3\ \mathbf{Tcal} - b4\ \mathbf{Tc} + \mathbf{TE} - (Ca - off)/\mathbf{G}$$

$$\mathbf{Ta} = c1\ \mathbf{T'a} - c2\ \mathbf{Tr}$$

where the coefficients are derived from the primary coefficients shown in figure 19. The brightness temperature is then derived from the antenna measurement, by accounting for the reflector losses and side lobe contributions.

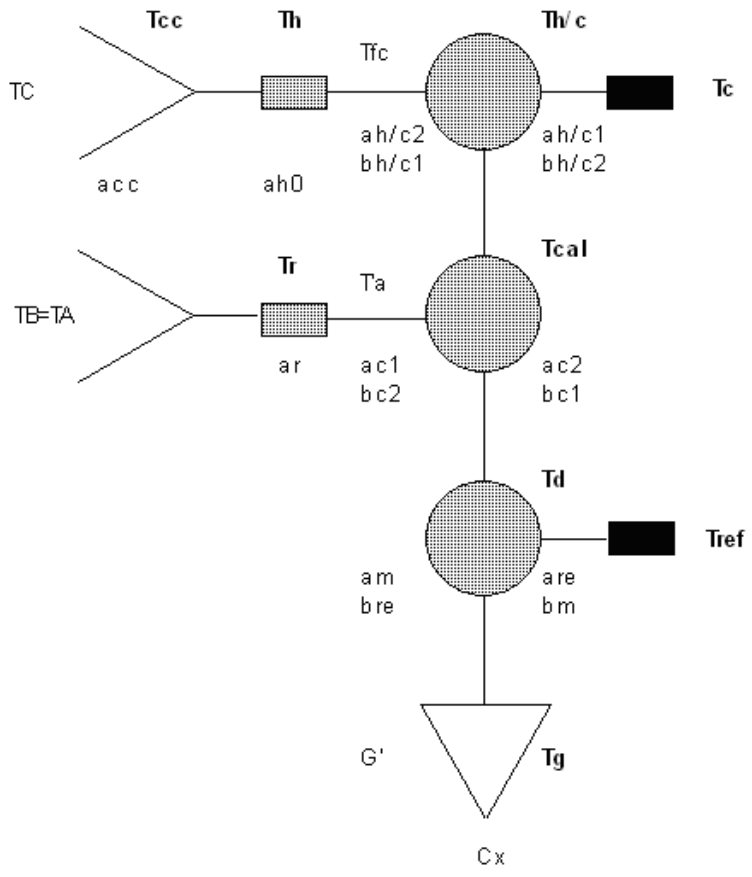

Figure 19: Scheme of one channel of the MWR, showing the main antenna, whose measurement is TA, the two calibration loads, consisting of an internal hot load and a sky horn, the reference load (Dicke load - temperature Tref) and internal switches to get every measurement. Each component is characterized by transmission and loss factors which are taken into account in the radiometer model, as well as their temperature.

B References

References

[1] Bernard et al, *The microwave radiometer aboard ERS-1: Part 1 - characteristics and performances*, IEEE Trans. Geosci. Remote Sensing, 31(6), 1186-1198, 1993.

[2] Eymard et al, *Intercomparison of TMR and ERS/MWR calibrations and drifts*, SWT TOPEX-JASON, New Orleans, Oct. 2002.

[3] Eymard et al, *Reports on activities performed in 2001 on the ERS2/MWR survey*, May 2002.

[4] Eymard et Obligis, *Preliminary report on long-term stability of ERS2/MWR over continental areas*, 1999.

[5] Obligis et al, *An assessment of ENVISAT/MWR measurements and products, Envisat QWG meeting*, 26-27 September 2005, Toulouse, France.

[6] Obligis et al, *Envisat/MWR: 36.5 GHz channel drift status*, March 2003.

[7] Ruf, *Detection of calibration drifts in spaceborne microwave radiometers using a vicarious cold reference*, IEEE Trans. Geosci. Remote Sens., 38(1), 44-52, 2000.

[8] Tran, Obligis, and Eymard, *Evaluation of Envisat MWR 36.5 GHz (updated status)*, CLS-DOS-NT-05-073 Report, 20 April 2005.

[9] Obligis, Labroue and Eymard, *Envisat/MWR : new calibration and generation of new consistent geophysical algorithms.*, CLS-DOS-NT-06-258 Report, 5 January 2007.